2021

Climate change impacts go beyond the surface: Groundwater recharge rates and aquifer resources across the Contiguous United States

Kendra R. Devereux

The College of Wooster, kdevereux21@wooster.edu

Climate change impacts go beyond the surface: Groundwater recharge rates and aquifer resources across the Contiguous United States

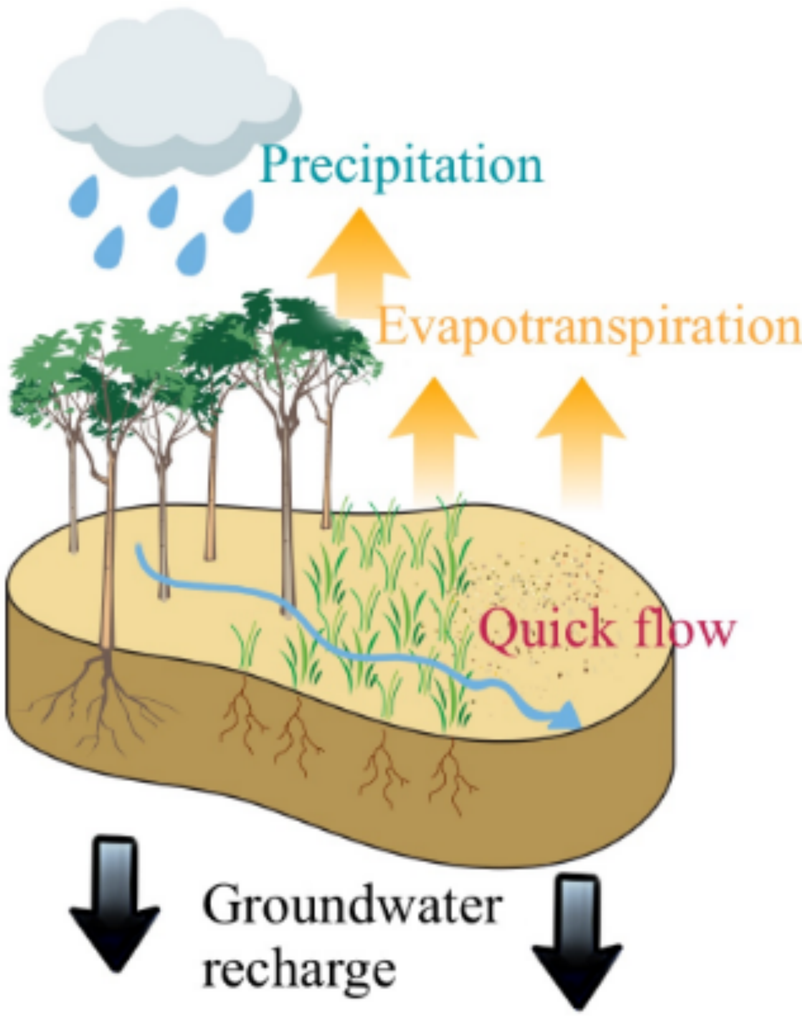

by
Kendra Devereux

Submitted in partial fulfillment of the requirements
of Senior Independent Study at
The College of Wooster

February 18, 2021

ABSTRACT

Groundwater is a primary source of potable water for millions and a major source for crop irrigation in the United States. Thus, it is vital to understand current and future rates of recharge to predict and manage groundwater availability. In this study, current groundwater recharge rates across the Contiguous US at 800m resolution are estimated by following methods presented by Reitz et al. (2017), and the reproducibility of the methods are assessed. A water budget approach is implemented where quick flow runoff and evapotranspiration rates are subtracted from precipitation rates. Precipitation was found to be the most reproducible water budget component, whereas evapotranspiration and quick flow runoff were found to be more sensitive aspects of the model. Final recharge estimates, dependent on the three water budget components, reflect inaccuracies produced in estimating precipitation, quick flow runoff, and evapotranspiration. Patterns in recharge rates are examined alongside the geospatial distribution of precipitation in the context of large-scale atmospheric circulation systems. In addition, changes to precipitation patterns that are expected to occur over the 21st century such as increasing precipitation in the Midwest and decreasing precipitation in the Southwest, are presented as a way of estimating changes to future groundwater recharge rates. Agriculture in the US relies heavily on groundwater resources, thus increased precipitation in the Midwest and decreased precipitation in the Southwest are expected the drastically alter US food production.

ACKNOWLEDGEMENTS

First and foremost, I would like to thank my advisor, Dr. Greg Wiles. I could not have done this without your guidance, care, and humor throughout! I further extend my thanks to everyone in the Earth Sciences department. I am forever indebted to the faculty and my fellow students for turning me into the scientist I am today.

I would also like to thank Dr. Chris Russoniello of West Virginia University. Thank you for entrusting me with this project as your REU student this past summer. And thank you to the entire Rutgers Ocean Data Labs REU program and the REU team's support!

I must also thank my coach, Amy Behrman. Coach, thank you from the bottom of my heart for all your care these past four years. Your genuine interest and encouragement in everything I do on and off the court is so deeply appreciated. To my teammates, I am so grateful for all the time we have spent together. Thank you for making Wooster feel like home.

Finally, thank you to my parents, my brother, and all of my friends. Your loving encouragement and words of reassurance have been so incredibly meaningful. Thank you!

TABLE OF CONTENTS

INTRODUCTION

Groundwater supplies potable water for millions and is a major source for crop irrigation in the United States. This important resource is stored in aquifers that are replenished through recharge, by which water percolates through the unsaturated zone and into aquifers. It is vital to understand current and future rates of recharge to predict and manage groundwater availability. Understanding the spatial distribution of groundwater recharge and how it is expected to change over time is especially important for water resource managers during present and anticipated changes in hydroclimate. High resolution spatial knowledge of groundwater recharge rates will help managers prepare for and mitigate the impacts of climate change on vulnerable populations that rely on groundwater.

Groundwater recharge rates can be calculated using a water budget approach by which quick flow runoff and evapotranspiration rates are subtracted from precipitation rates. Given the tight relationship between precipitation and recharge, precipitation patterns governed by large-scale atmospheric circulation systems directly influence the spatial availability of groundwater resources. Estimating future groundwater recharge rates therefore involves understanding the likely changes in atmospheric circulation and resulting precipitation patterns that will occur and using climate models to make future estimates of each water budget componenet.

The initial goals of this study were to (1) estimate groundwater recharge rates across the Contiguous US (CONUS) at 800 m resolution by following the methods presented by Reitz et al. (2017) and to (2) apply the same methods to estimate future groundwater recharge rates across the CONUS using Climate Model Intercomparison Project Phase 5 (CMIP5) precipitation and temperature projections. In this study, the first goal is fulfilled, but time constraints prevented fulfilment of the second goal, which has been modified as described below.

The water budget approach where quick flow runoff and evapotranspiration are subtracted from effective precipitation is used to estimate current groundwater recharge rates. The three water budget components of precipitation, quick flow runoff, and evapotranspiration were calculated using previously developed regression equations developed using historical datasets (Reitz et al., 2017), including atmospheric, geologic, and land cover data. The reproducibility of the methods presented by Reitz et al. (2017) is also assessed here.

Probable changes to precipitation patterns across the CONUS over the 21st century are presented in this study because of their tight relationship with recharge rates. As such, case studies of regional changes to precipitation and changing patterns over the Midwest and the Southwest are examined. The Midwest is expected to experience the greatest increases to precipitation due to an intensifying polar jet stream while the Southwest is expected to experience the greatest decreases to precipitation in part due to the poleward migration of Hadley Cells (Zhang and Villarini, 2019; Seager et al., 2007). Changing water resources in these regions are essential to monitor due to their importance as a water supply and in crop production. The Midwest produces about 70% of the country's corn and the Southwest produces about 40% of the country's fruits (USDA, 2014; USGS, 2020). Midwestern farms are expected to experience problems related to oversaturated soils and flooding, which will negatively impact corn production. Southwestern farms are expected to experience depleting aquifers, which will negatively impact fruit production capacity.

BACKGROUND

Groundwater and its importance

Groundwater, as its name suggests, is water that is located in the ground, stored in the saturated zone below the water table where all pores in the soil and rock are completely filled with water. The saturated zone can also be referred to as aquifers, which are defined as stores of water that can be used by people. In the United States, groundwater, as stored in aquifers, provides a crucial source of potable drinking water and irrigation. Millions of people in the US rely on groundwater in their daily lives, making the management of groundwater highly important to their health and livelihoods (USGS, 2015).

Water replenishes aquifers through the process of groundwater recharge, in which water infiltrates downward through the ground. Precipitation, evapotranspiration, and overland runoff, or quick flow, are all factors that determine groundwater recharge rates and spatial variability (USGS, 2015). As people withdrawal water from aquifers, recharge replenishes the aquifers, although usually at lower rates. Changes to any of these factors, as well as rates of water withdrawal, are important to monitor so that water resource planners can predict changes in water availability in their aquifers.

Current assessments of groundwater use in the US indicate that many regions are using groundwater at an unsustainable rate (Purdue Policy Research Institute, 2018). Unsustainable here refers to where withdrawal rates from aquifers exceed recharge rates. Many of the regional aquifers experiencing highly unsustainable groundwater extraction rates in the western and central United States include the High Plains Aquifer (also known as the Ogallala aquifer), the Central Valley of California, the Snake River Basin Aquifer, and the Washington State Aquifer. (Figure 1). Currently, there are no restrictions on groundwater withdrawals from the High Plains, Snake River Basin, or Washington State aquifers, and restrictions of withdrawals from the Central Valley aquifer only began in January of 2020 (California Department of Water Resources, 2020). Anticipated increasing groundwater demand will only increase stress into the future.

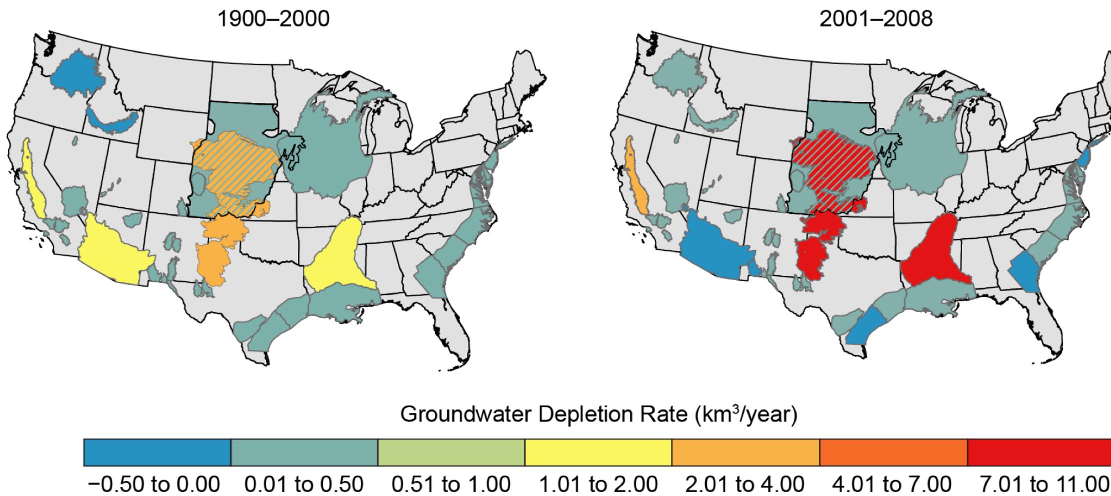

Figure 1. Groundwater depletion rate per year of the United States' major aquifers, including the High Plains, Central Valley, Snake River basin, and Washington aquifers. Depletion rates have increased as agricultural demands have increased over time. (From the US Global Change Research Program, 2018)

Groundwater stresses and agriculture

Scanlon et al. (2012) found that about 330 km^3 of water has been depleted from the High Plains aquifer since 1950. This depletion is almost 36% of the total estimated water storage declines in all aquifers of the US since 1900 (Scanlon et al., 2012). The High Plains aquifer is in a region often called the "grain basket" of the United States because it produces nearly 50 million tons of grain each year, and this production depends on the aquifer for 90% of the irrigation it needs (Mrad et al., 2020). Scanlon et al. (2012) reports that 140 km^3 of water has been depleted in the Central Valley aquifer of California since the 1860s. Since 1900, the Central Valley depletion accounts for approximately 15% of the total estimated water storage declines in all US aquifers. The Central Valley aquifer is sometimes called the United States' "fruit and vegetable basket", producing 40% of the nation's fruits and vegetables (USGS, 2020). Together, depletion of the High Plains and Central Valley aquifers account for 51% of the total estimated US groundwater storage decline. Since these two regions produce enormous amounts of our nation's fruit, vegetables, and grains, the large and continuous decline in storage presents a substantial risk to our nation's food security.

Although this storage decline of 51% refers to the total decline of US water sources since 1900, the depletion has not been steady through time. For the High Plains aquifer, depletion has increased over time, however, the Central Valley aquifer depletion has occurred episodically, with the largest drawdowns coinciding with major droughts superimposed on a steady decline. During droughts, reductions in recharge to the aquifer can fall by 60% (Scanlon et al., 2012). Thus, future water supplies in the western United States are expected to be further stressed by climate change with less general water availability and a likely increase in drought conditions (IPCC, 2014).

The Purdue Policy Research Institute (2018) predicts that many of the challenges involving unsustainable groundwater use will lie in food production. On top of the unsustainable groundwater practices currently occurring, global population and income growth are two factors that will continue to place pressure on our water resources. Population and income growth, both in the United States and in other parts of the world such as India and China, are expected to drive ¼ of US cropland expansion in the coming decades. However, the current unsustainable groundwater use practices occurring in the US mean that restrictions must be placed on future groundwater withdrawals, which then presents a problem for the anticipated cropland expansion.

The Purdue Policy Research Institute (2018) suggests that the inevitable outcome will be shifting global crop production overseas as well as to new areas within the US.

As described, US agriculture relies heavily on groundwater aquifers and is highly important for national and global food production. Changes in groundwater recharge rates over time and its spatial variability due to climate change will only exacerbate the current groundwater stresses agricultural regions are experiencing due to unsustainable groundwater use. Thus, monitoring the rapidly depleting aquifers used to support agriculture, monitoring groundwater recharge rates, and predicting how recharge rates will change in the future is extremely important as a climate change mitigation strategy.

Climate and recharge

Current groundwater recharge rates can be estimated based on relative amounts of precipitation, evapotranspiration, and quick flow runoff inferred from a region's known climate. This is a water budget approach to calculating recharge, where evapotranspiration and quick flow runoff are subtracted from precipitation. The value that remains is attributed to groundwater recharge. Therefore, in order to calculate recharge rates, rates of evapotranspiration and quick flow runoff need to be calculated first. To calculate these water budget components of evapotranspiration and quick flow runoff, values for annual precipitation rates and temperature must be incorporated.

The following sections first examine recorded values of historic precipitation and temperature, placing current water budget components in a long-term context. Then, estimates of future climate change in terms of how precipitation and temperature are predicted to change over the 21st century are considered.

Recorded climate change

Historic precipitation trends

Historical variations in precipitation, measured through both instrumental and proxy records, determine how future precipitation is projected. This is possible because these historical datasets are used to calibrate models that anticipate future changes. From these historical records, annual precipitation averaged across the US has gone up around 4% over 1901-2015 (Easterling et al., 2017). Regionally, however, there are strong differences, with the Northeast, Midwest, and Great Plains having experienced increases while much of the Southwest and Southeast have experienced decreases. There are also seasonal differences; fall has had the greatest national increases while winter has remained mostly unchanged (Easterling et al., 2017; Figure 2). Future regional and seasonal differences, although beyond the scope of this study, are important to keep in mind when predicting future annual averages of precipitation.

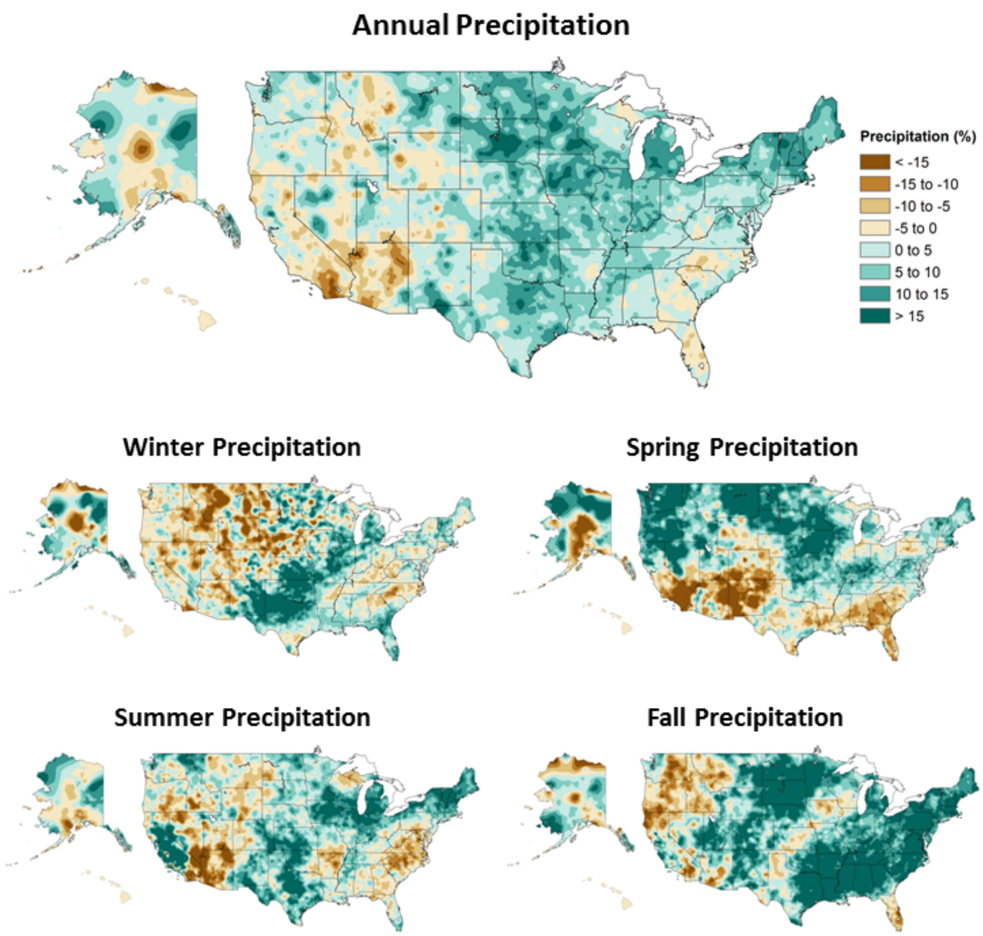

Figure 2. Annual and seasonal changes to present-day (1986-2015) precipitation relative to precipitation averaged over 1901-1960. Regional changes, such as the increase to precipitation occurring in the eastern half of the CONUS, can be observed. Seasonal changes, such as the general increases occurring in the fall, can also be observed. (From Easterling et al., 2017, Figure 7.1).

In addition to observed changes in total precipitation, there have also been changes in extreme precipitation events. Because extreme events occur when the air is nearly completely saturated with moisture, and more moisture can be held in warmer air than cooler air, they generally increase in intensity by around 6% per degree Celsius temperature increase (Easterling et al., 2017). As with total precipitation, there are regional differences in the increase of extreme events. The northeastern US has experienced the greatest increase in extreme events at 27%

since 1901. In contrast, the western US has had relatively small increases in extreme precipitation events and even some slight decreases (Easterling et al., 2017).

Historic temperature trends

Warming throughout the 20th century has not been constant. In general, there was a warming period from 1895 until about 1940, a cooling period from 1940-1970, and a final, more rapid warming period from 1970 to the present. Since the warming has not been constant, trends in historic temperature have been calculated using different methods and have therefore yielded different results; however, the consensus on annual average temperature increase over the CONUS from 1895-2016 spans a range of 0.7-1.0 °C (Vose et al., 2017).

Like the observed and predicted trends in precipitation, there are regional and seasonal differences in temperature trends. Overall, warming was minimal (less than 0.3 °C) along coastal areas and largest over more interior regions. The greatest warming occurred in the Northwest, the Southwest, and the Northern Great Plains, with increases above 0.8 °C. The Southeast had the smallest amount of warming. Seasonally, warming was greatest in the winter months and smallest in the summer. In the winter, some regions experienced temperature increases of over 0.8 °C. Exhibiting the high variability in the observed trends, some cooling was in fact noted during the summer months for parts of the Southeast, Midwest, and Great Plains (Vose et al., 2017; Figure 3).

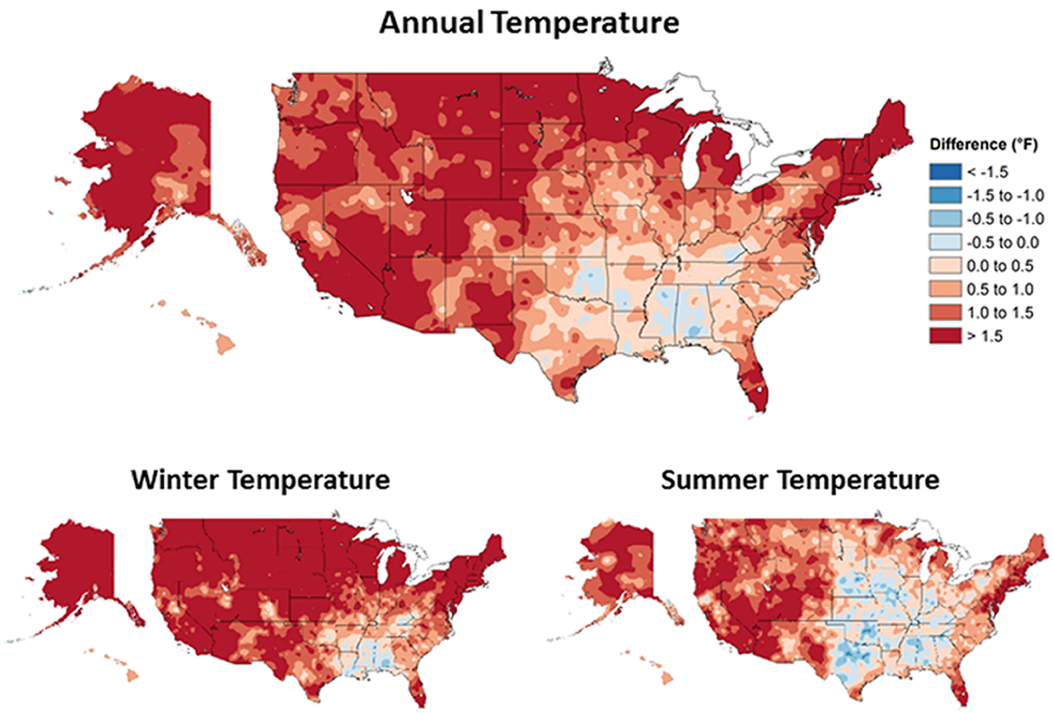

Figure 3. Annual, winter, and summer temperature changes from 1986-2016 relative to 1901-1960. The least amount of warming has occurred in the southeast and the greatest amount of warming has occurred in the Northwest, Southwest, and Great Plains regions. (From Vose et al., 2017, Figure 6.1).

Temperature extremes, which can also impact hydroclimate, exhibit historical changes as well. Cold extremes have become less severe over the 20th century, evident in the observation that the coldest daily temperature of each year has risen consistently over the CONUS. In addition, cold nights – those with a minimum temperature below the 10th percentile from 1961-1990 – have declined in all regions of the CONUS. Warm extremes, on the other hand, increased in parts of the West, observed as increases to the warmest daily temperature of the year. However, many regions in the East did not experience greater warm temperature extremes, exhibiting the more nuanced regional pattern seen for warm temperature extremes compared to cool temperature extremes. Nationwide, there has been a slight increase in the number of droughts and heatwaves (Vose et al., 2017).

Future climate change

Representative Concentration Pathways

Anticipating future changes in hydroclimate rely on model predictions. Representative concentration pathways, or RCPs, are climate change scenarios which include a time series of emissions and the concentrations of greenhouse gases for a given scenario. RCPs are "pathways" in that they provide time-dependent projections of greenhouse gases in the atmosphere. In addition, the term "pathway" emphasizes that RCPs do not only produce a specific long-term radiative forcing outcome, but also explain the trajectory that would be taken to reach that outcome. RCPs are "representative" in that each RCP provides only one of several possible trajectories that would each lead to their own specific radiative forcing outcome (Moss et al., 2008).

The term "radiative forcing" refers to the change in the net radiative flux at the top of the atmosphere – the tropopause – due to a change in an external driver of climate change. Energy is constantly flowing into the atmosphere. Some of the energy is reflected back off of Earth and the rest of this energy is absorbed by the Earth. If subtracting the energy flowing out from the energy flowing in gives a positive number, then the Earth must be warming. Changes to the way the atmosphere is absorbing the sun's energy can change the radiative flux to cause a radiative forcing. For example, a change in the concentration of greenhouse gases in the atmosphere, such as carbon dioxide or methane, causes an increase to the radiative flux applied to the atmosphere. This increase to the radiative flux creates a positive radiative forcing. An increase in the output of the sun would also cause an increase to the radiative flux, leading to a positive radiative forcing. Radiative flux is defined as the amount of power radiated through a given area, with radiative forcing measured in watts per square meter or W/m^2.

Four RCPs are commonly used by the climate modelling community. There is one high radiative forcing pathway – RCP8.5 – in which radiative forcing reaches 8.5 W/m^2 by 2100 and continues to rise beyond 2100. There are two medium or "stabilizing" pathways – RCP6.0 and RCP4.5 – in which radiative forcing reaches 6.0 W/m^2 and 4.5 W/m^2 respectively by 2100 and stabilizes at those levels. Finally, there is one lower radiative forcing pathway – RCP2.6 – in which radiative forcing peaks around 3.0 W/m^2 before 2100 and then declines (Moss et al., 2008).

The original second goal of this study was to use RCPs to project groundwater recharge rates into the future. Although the results presented in this study were unable to fulfill this second goal, future work will focus on using future climate projections and fulfilling the second goal. Two of the four RCPs will be considered in future work, RCP8.5 and RCP4.5. The high radiative forcing pathway will be used because it represents a scenario where greenhouse gas emissions continue to rise throughout the 21st century without slowing down. This is a "business as usual" scenario and is the pathway we are currently on. The moderate radiative forcing pathway, RCP4.5, will also be considered. The low-radiative forcing scenario RCP2.6 is not considered because global emissions have now reached a level that renders it nearly impossible. In order to follow the RCP2.6 scenario, emissions would have had to peak around 2020 and then immediately start declining (Moss et al., 2008). In the year 2021, with the year 2020 reported as tied with 2016 for the warmest year on record (NASA, 2021), there is no sign that global emissions will be slowing down anytime in the near future.

Future precipitation projections

Estimates of future precipitation over the CONUS that will be used in the future of this study come from the Coupled Model Intercomparison Project Phase 5 (CMIP5) simulations. These models describe a mix of both increases and decreases to seasonal and regional precipitation changes. These precipitation estimates are expected to translate into respective groundwater recharge increases and decreases given their close relationship through the water budget approach to measuring recharge.

Anticipated future seasonal average precipitation patterns are regionally and seasonally dependent. For example, there will likely be increases to winter and spring precipitation in the northern US, first as snow and then, with increasing warming, as rain. In contrast, the southwestern US will experience slight decreases to spring precipitation (Easterling et al., 2017; Figure 4).

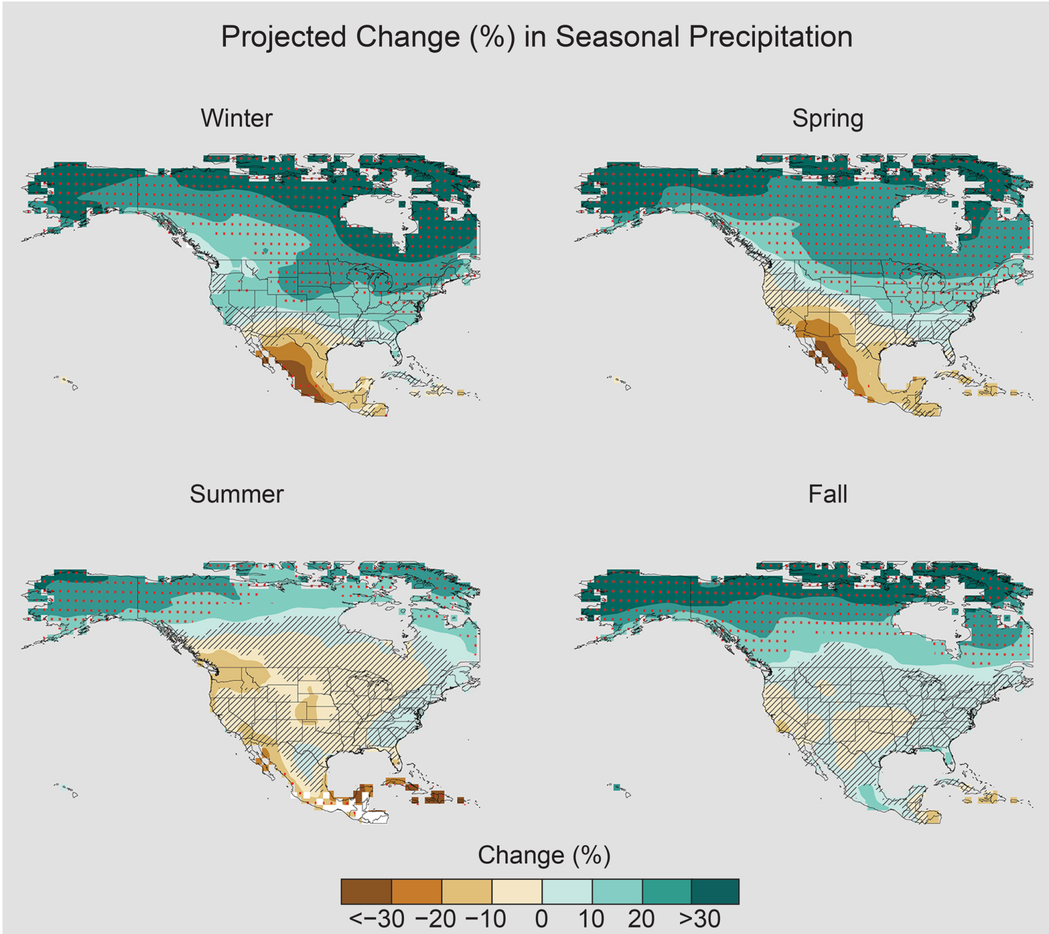

Figure 4. Projected percent change in seasonal precipitation for 2070-2099 relative to the 1976-2005 average under RCP8.5, the high emissions scenario. Dotted regions indicate the projected changes are large compared to natural variation and hashed regions indicate the projected changes are small compared to natural variation. (From Easterling et al., 2017, Figure 7.5).

Although the mean changes in seasonal precipitation are difficult to predict given the uncertainty of changing large-scale circulation patterns over the CONUS, confidence is high that there will be an increase in the frequency and intensity of extreme precipitation events. Increases to extreme precipitation events are expected in all regions, including regions where total precipitation is expected to decline, such as the southwestern US. Under the high emissions scenario (RCP8.5), extreme events are expected to become two to three times more frequent by

2100. As in the historical increases to extreme precipitation, the greatest increases are expected for the northeastern US (Easterling et al., 2017).

Future temperature projections

Estimates for future temperature come from the Coupled Model Intercomparison Project Phase 5 (CMIP5) simulations. From these simulations, it is expected that extreme temperatures will increase more than average temperatures (Vose et al., 2017).

Annual average temperatures will increase over the 21st century, but the amounts vary dramatically for the different RCP scenarios. The RCP4.5 scenario projects an increase of around 2.8 °C while the RCP8.5 scenario projects an increase of around 4.8 °C by 2100. All RCP scenarios include a wide range of likely temperature increases (1.6-4.1 °C for RCP4.5 and 3.2-6.6 °C for RCP8.5), representing the average increase for the three coldest months and the average increase for the three warmest months. Overall, greater temperature increases are expected for summer than for winter. Regionally, higher latitudes will continue to warm at faster rates relative to lower latitudes. For example, the Northeast is expected to warm 5.5 °C by 2100 under RCP8.5 compared with a projected warming of 4.2 °C for the Southeast under RCP8.5 (Vose et al., 2017; Figure 5).

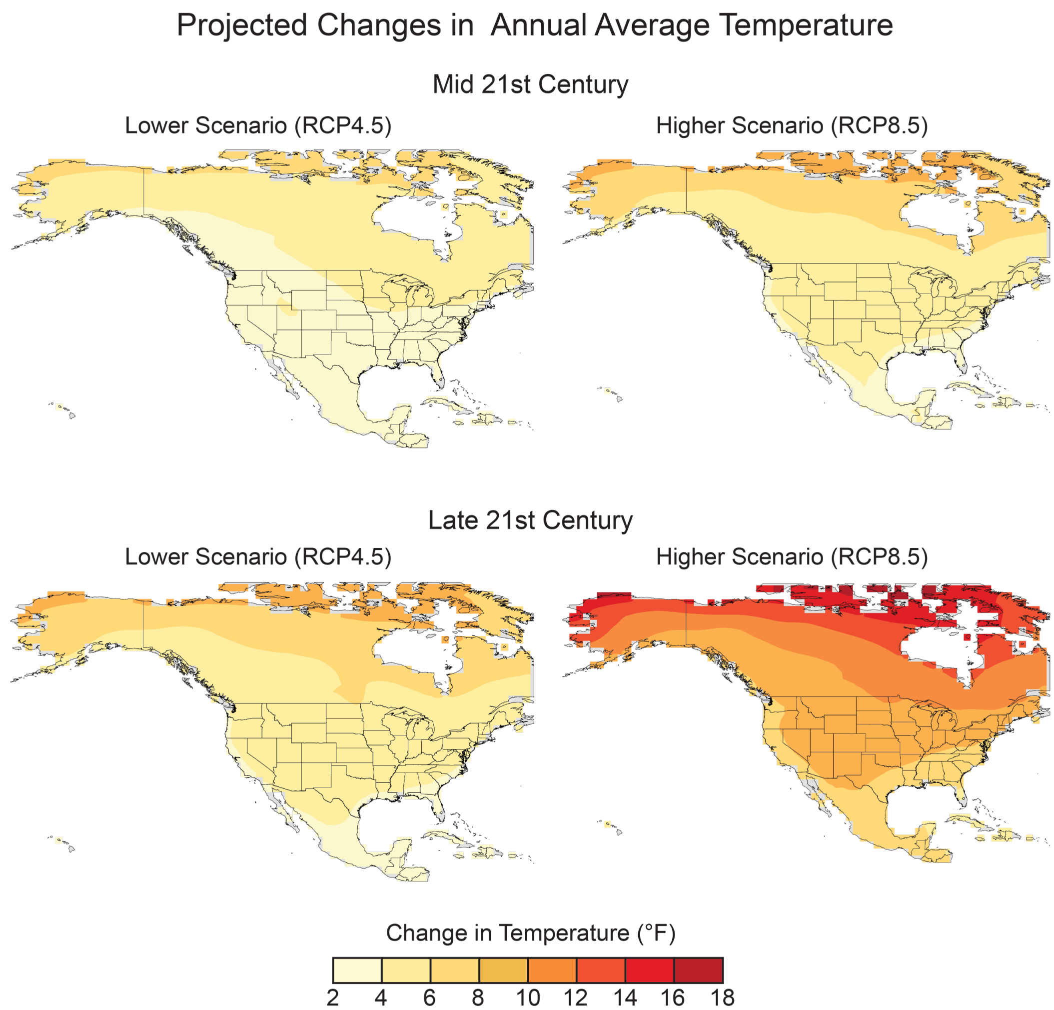

Figure 5. Projected changes in annual average temperature for mid-century (2036-2065) and late-century (2070-2099) compared to the near-present (1976-2006) average. Drastic differences can be seen between RCP4.5 and RCP8.5. (From Vose et al., 2017, Figure 6.7).

Under the strongest warming scenario (RCP8.5), temperature extremes are going to increase dramatically. Current 1-in-20-year maximum temperatures are projected to occur every year and current 1-in-20-year minimums are not going to occur at all by the end of the century. In addition, there will be larger increases to the coldest temperature of the year relative to the warmest temperatures of the year. As with annual average temperatures, the northern half of the CONUS is expected to warm more drastically than the southern half, experiencing the greatest increases to the lowest temperatures of the year. Cold waves will become less frequent and less intense, while heat waves are going to become more frequent and more intense. Under RCP8.5, heat waves will have temperature increases of at least 6.1 °C nationwide. Finally, there will also be dramatic increases to the number of days over 90 °F, where an additional 20-30 days annually is expected for most of the country, with some parts of the South experiencing increases of 40-50 days annually (Vose et al., 2017).

The 100th meridian

The 100th meridian is a line of longitude (Figure 6) that cuts through the states of Texas, Oklahoma, Kansas, Nebraska, and the Dakotas. This boundary roughly corresponds to a division between the arid western United States and the more humid Eastern United States. Moving east to west across the 100th meridian displays a gradual shift from rolling prairies of green grasses to barren ground with only sparse vegetation (Seager et al., 2018).

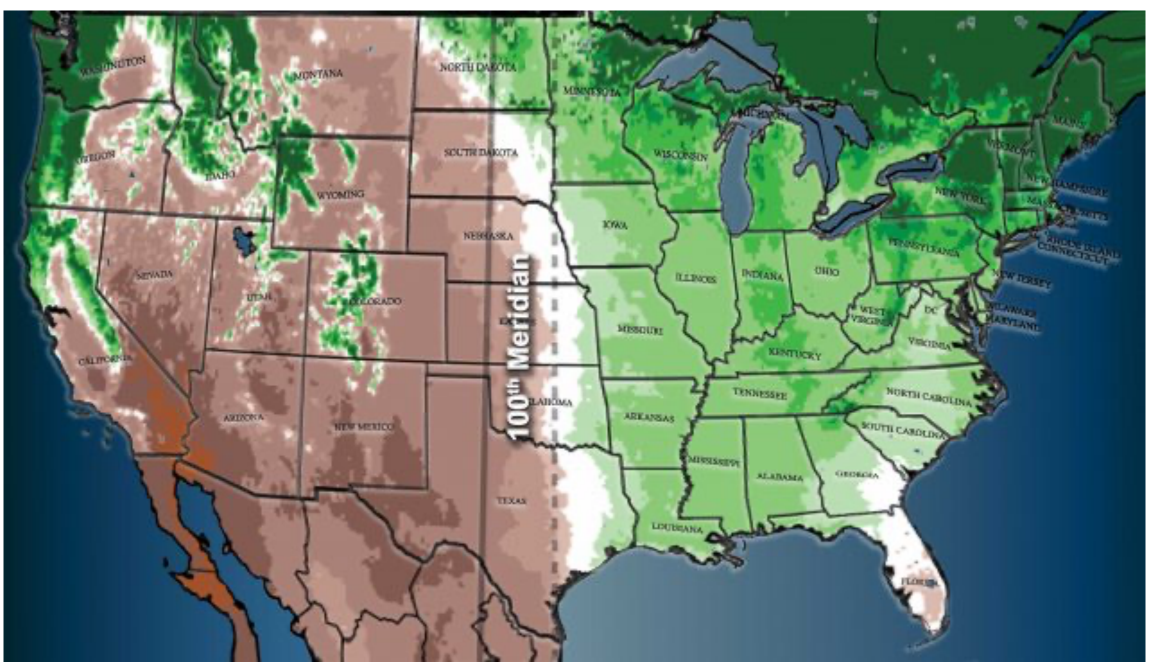

Figure 6. The divide between an arid western US and a wetter eastern US falls at the 100th meridian (Figure from Lamont-Doherty Earth Observatory, 2018).

The climate divide along the 100th meridian is the result of global-scale wind patterns that causes rainfall to decrease sharply to the west of the meridian and increase sharply to the east of the meridian. The western plains are dry partly because they lie in a rain shadow caused by the Rocky Mountains, which capture most of the moisture blowing from the Pacific Ocean. In addition, winter storms bring moisture to the eastern US from the Atlantic, but they do not travel far enough to reach the western plains. Finally, summer moisture is provided to the eastern US from the Gulf of Mexico. This moisture travels eastward, again acting only as a moisture source for the east (Seager et al., 2018).

In the future, it is predicted that the arid-humid climate divide historically located over the 100th meridian will slowly begin shifting eastward as a result of climate change (Seager et al., 2018). Rising temperatures are causing increasing evaporation rates over the plains, while changing wind patterns are causing less rain to fall in the southwest (Seager et al., 2018). This will result in the easterly expansion of the arid western plains. Parts of the Midwestern-Central US, which historically has a humid climate, may gradually become more arid. Data collected since the 1980s shows that the climatic divide between the arid west and the humid east has already shifted some 140 miles eastward, placing the new climatic divide closer to the 98th meridian. So far, this change has not resulted in any large-scale land use changes, but the eastward migration of the climatic divide is expected to continue throughout the 21st century (Seager et al., 2018). Eventually, changes to the historical climatic regime will be large enough to have major implications for agriculture.

Researchers predict that some farms in the Central to Midwestern US will need to adapt as the climatic divide shifts eastward (Seager et al., 2018). For example, they may need to become larger in order to keep the same productivity levels under a more arid climate. In addition, if farmers want to continue growing crops that require moist conditions, such as corn, they will need to implement irrigation systems to ensure their crops receive enough moisture. If irrigation is not implemented, farms may instead need to switch to growing crops more suitable for arid conditions, such as wheat (Seager et al., 2018). Currently, farms to the west of the 100th meridian largely produce wheat due to the crop's tolerance for aridity, or else use land as grazing fields for livestock. It is therefore expected that more and more farms in the Midwest will adopt these agricultural practices typical of western states in order to keep up with changing conditions (Seager et al., 2018).

In addition to difficulties arising for agricultural areas, urban areas in parts of the Midwest will also face some challenges due to the eastward migration of the 100th meridian climatic divide. Water supply to cities and homes may decrease as the climate becomes drier. This concern echoes the same concerns that the original identifier of the 100th meridian, John Wesley Powell, had in the late 1800s (Lamont-Doherty Earth Observatory, 2018). Powell was worried about sufficient water supply to large-scale developments in the harsh conditions of the arid western United States. He even tried convincing Congress to lay out the necessary water management districts to help prepare settlements for the constraints on water resources in the west. Political leaders did not listen to Powell, leading to problems with the development of the western US. Similar problems due to decreased water supply in the Midwest are expected to emerge throughout the 21st century (Lamont-Doherty Earth Observatory, 2018).

Drying of the Midwest due to the shifting 100th meridian contradicts predictions for a wetter Midwest due to intensifying large-scale circulation patterns that have been bringing more and more precipitation to the Midwest over the 20th century (Easterling et al., 2017). The 100th meridian has so far only shifted 140 miles east. This demonstrates the spatial variability and complexity involved in predicting changing precipitation patterns and may indicate that changes will not be able to be generalized for an entire region. For example, parts of the Midwest closest to the 100^{th} meridian and the Central US, such as in Kansas, Nebraska, and the Dakotas, may experience some drying as the climatic divide begins moving slowly east. On the other hand, states in the Midwest farther from the 100^{th} meridian such as Ohio, Michigan, and Indiana may experience wetter conditions from changing circulation patterns. Given the spatial intricacies involved in predicting future climate change, high resolution maps of water budget components are necessary because of their ability to provide more localized information.

METHODS

This project focuses on replicating the methods of Reitz et al. (2017), which estimated annual groundwater recharge rates averaged over 2000-2013 for the CONUS. The recharge is based on hydroclimate and geologic material inputs following the procedure of Reitz et al. (2017). Results presented here are then compared with those of Reitz et al. (2017) in order to examine the method's reproducibility.

Estimating groundwater recharge rates involves first producing estimates of the three water budget components of precipitation, evapotranspiration, and quick flow. Quick flow refers to surface runoff, which is separated from baseflow. We used regression equations produced by Reitz et al. (2017), to calculate these three components of the water budget. Then, the three components were used in the overall water budget equation to calculate recharge:

$$R = P - ET - Qf \tag{1}$$

Estimating near-present annual groundwater recharge rates

Precipitation

The first water budget component calculated was annual precipitation using methods laid out by Reitz et al. (2017). The annual precipitation data used came from the PRISM Climate Group at Oregon State University, which provides precipitation estimates at an 800m resolution for the 1981-2020 30-year normal (prism.oregonstate.edu). These data are in a calendar year format. Therefore, the rest of the water budget components are also treated in a calendar year format rather than by water year.

Irrigation is also considered in the precipitation component of the water budget. In some parts of the country, such as the drier parts of the West, irrigation for crops and golf courses contributes greatly to the water available for evapotranspiration, quick flow, and recharge, thus it is a necessary consideration in the water budget. Irrigation data by county comes from the 2010 USGS Water Use data set (Maupin et al., 2014). The data has separate categories for fresh groundwater withdrawals and surface water withdrawals. Only the groundwater-sourced irrigation withdrawals are considered in this study because this groundwater comes from deeper aquifers that are not hydrologically connected to streamflow. Therefore, groundwater-sourced irrigation represents an addition to the water budget, whereas if the surface water withdrawals were to be included in the water budget, the volume of water estimated would effectively be double counted.

Irrigation values by county for all states were applied to areas classified as either "agriculture" or "open urban" by the 30m resolution Landsat-derived 2006 National Land Cover Database (NLCD, 2011 edition of the 2006 map, https://www.mrlc.gov/data) for crop and golf course irrigation. Contributions from irrigation were capped at 1 m/year because values greater than this are usually the result of mismatches between land-cover-designated agricultural area and county-reported agricultural irrigation.

Using Equation 1 from Reitz et al. (2017), the effective precipitation was calculated:

$$P = P_0 + IR \tag{2}$$

Equation 2 represents effective precipitation, where the PRISM Climate Group's annual precipitation data (P_0) is added to the groundwater-sourced irrigation for crops and agriculture (IR). P hereafter will refer to this effective precipitation.

Evapotranspiration

A regression equation (Equation 3) developed by Reitz et al. (2017) was used to calculate annual average evapotranspiration (ET) at 800m resolution over the CONUS:

$$\frac{ET}{P} = \frac{\Lambda(\frac{\Delta T}{\Delta \overline{T}})(\frac{T+C_1}{\overline{T}+C_1})^2}{\left(\frac{\Delta T}{\Delta \overline{T}}\right)\left(\frac{T+C_1}{\overline{T}+C_1}\right)^2+(\frac{P}{\overline{P}})^{\frac{3}{2}}} \tag{3}$$

Where T is the mean annual temperature (°C) and ΔT is the mean daily temperature maximum minus temperature minimum (°C), P is the effective precipitation (m/year, from Equation 2), and ET is evapotranspiration rate (m/year). Where $\overline{T}, \Delta\overline{T},$ and $\overline{P}$ appear, they are not fitting coefficients, but values averaged across all points collected from the calibration dataset of 2000-2013. Λ is a term describing the land-cover distribution:

$$\Lambda = 1 + aL_u + bL_f + cL_s + dL_g + fL_a + gL_m \tag{4}$$

Where L_u is the areal fraction urban, L_f is the fraction forest, L_s is the fraction shrubs, L_g is the fraction grassland, L_a is the fraction agriculture, and L_m is the fraction marsh. Boolean rasters were made to describe the areal fraction of the CONUS for each land-cover type with a “1” for areas with a given land-cover type and a “0” for areas without that land-cover type (Figure 7). Data for land-cover distribution comes from the 30m resolution Landsat-derived 2006 National Land Cover Database (NLCD, 2011 edition of the 2006 map, https://www.mrlc.gov/data). The fitting coefficients for each of the land-cover type areal fractions in Equation 4 are: a = 0.0526, b = 0.242, c = -0.0106, d = 0.236, f = 0.325, g = 0.520. The fitting coefficient C_1 in Equation 3 is 15.9. The built-in Python package “Arcpy” was used to run this equation and the script used is presented in Appendix A.

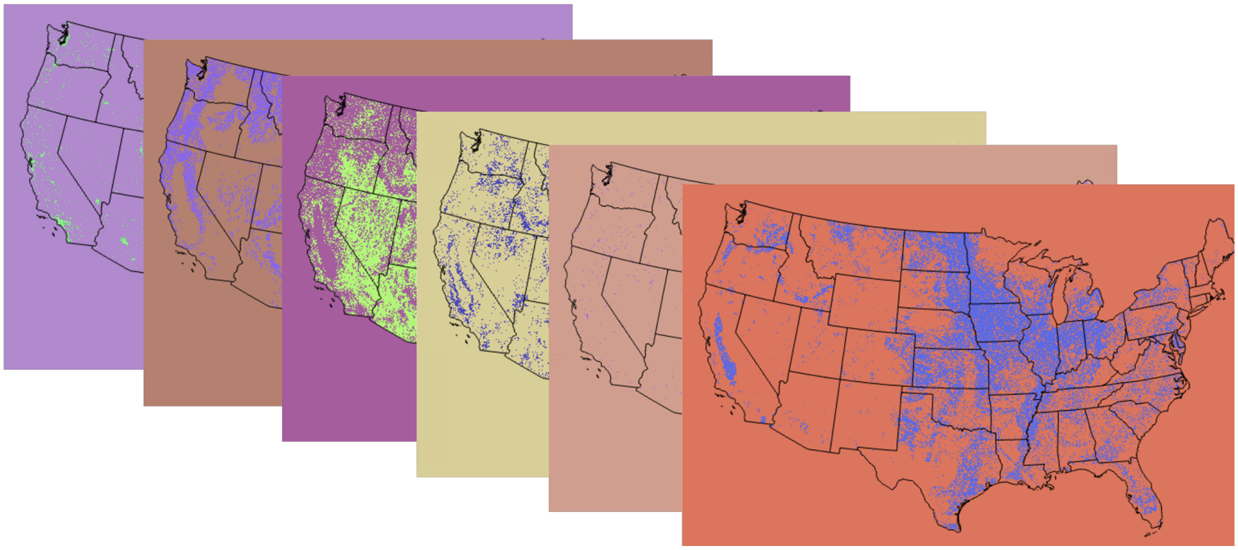

Figure 7. Boolean rasters were created for each land-cover type going into the Λ variable of Equation 3. Each colored dot for each layer is where a "1" appears, representing the presence of a given land cover type. From left to right, the stacked screen captures show areal fraction of urban, forest, shrubs, grassland, marsh and agriculture.

Quick flow

A map of surficial geology type was used as an explanatory variable for calculating quick flow. The map of surficial geology incorporated was adapted from Soller et al. (2009), which reduced the spatial coverage to fewer surficial geology categories (Figure 8). There are 16 surficial geology types considered.

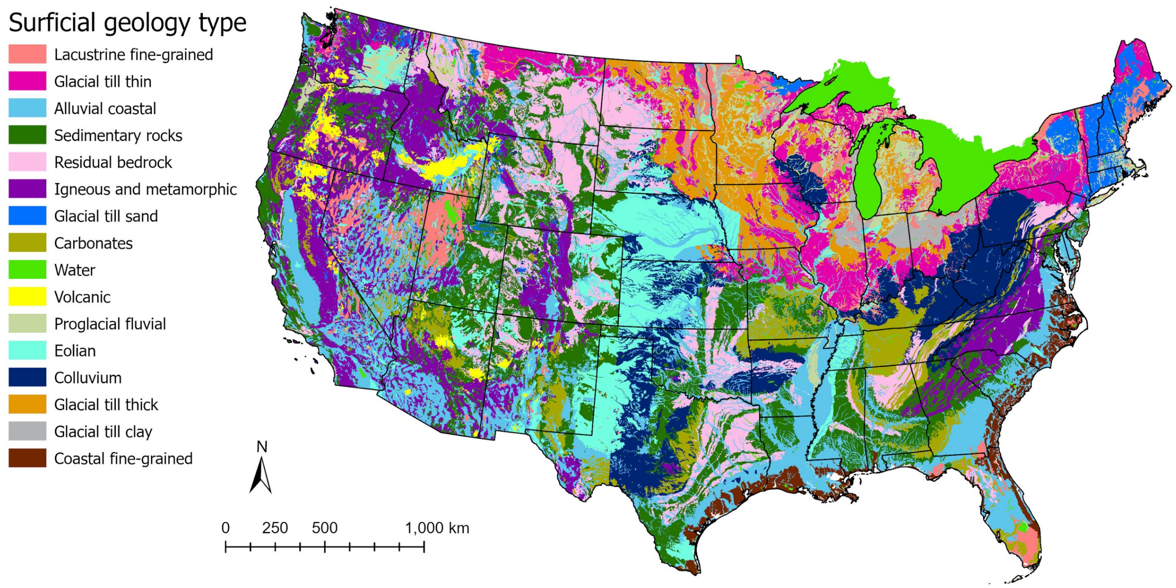

Figure 8. Surficial geology types incorporated in the quick flow regression (adapted from Soller et al., 2009).

The surficial geology categories (Figure 8) are included as fitting parameters in the regression equation. The regression equation (Equation 5) developed by Reitz et al. (2017) was used to calculate annual average quick flow measurements:

$$R_g = C_1 g \left(\frac{P}{\bar{P}}\right)^{a_g} \left(\frac{K}{\bar{K}}\right)^{b_g} + C_2 g \qquad (5)$$

In Equation 5, R_g is quick flow in m/year for a given surficial geology type, P is precipitation in m/year and K is saturated hydraulic conductivity in µm/s. Saturated hydraulic conductivity comes from the STATSGO database compiled by the US Department of Agriculture's Natural Resource Conservation Service (USDA, 2019, http://websoilsurvey.nrcs.usda.gov). $\bar{P}$ and $\bar{K}$ are averages of the effective precipitation and hydraulic conductivity datasets where $\bar{P} = 0.8022$ m/year and $\bar{K} = 19.99$ µm/s. The fitting parameters $C_1 g$, a_g, b_g, and $C_2 g$ are unique for each surficial geology type and are listed in

Table 1. The *Model Builder* feature in ArcGIS Pro 2.5 was used to run Equation 5, and is explained further in Appendix B.

Table 1. Fitting parameters for Equation 5 for each surficial geology type of Figure 1. From Reitz et al. (2017) Table 1.

Surficial Geology Type	C_{1g}	a_g	b_g	C_{2g}	R^2
Glacial till clay	0.1176	4.837	−0.7887	0.05168	0.67
Water	0.2197	1.325	−0.2432	−0.06081	—
Glacial till sand	0.2076	1.275	−0.2529	−0.03741	0.66
Glacial till thick	0.2087	4.779	−0.4416	0.01653	0.83
Glacial till thin	0.3228	1.150	−0.1674	−0.1408	0.85
Volcanic	0.08879	2.066	−0.2729	−0.0006759	0.83
Eolian	0.1652	2.613	−0.3711	−0.008208	0.85
Sedimentary rocks	0.2032	1.430	−0.2266	−0.05376	0.83
Colluvium	2.409	0.1403	−0.01533	−2.212	0.50
Residual bedrock	0.2170	1.385	−0.2641	−0.05877	0.84
Coastal fine grained	0.003102	7.459	−1.485	1.387	0.75
Proglacial fluvial	0.6749	0.4821	−0.0601	−0.4864	0.65
Carbonates	0.1470	1.802	−0.4601	−0.02143	0.70
Lacustrine fine grained	0.2343	1.249	−0.3252	−0.06878	0.74
Alluvial coastal	0.2021	1.452	−0.2629	−0.05542	0.78
Igneous and metamorphic	0.1548	1.606	−0.2166	−0.01827	0.83

Recharge

The estimate for recharge is the remainder of precipitation that was not taken into account with the quick flow or ET terms. The recharge component closes the water budget by estimating the contribution to baseflow. Therefore, the equation for calculating recharge uses a water budget approach (Equation 1):

$$R = P - ET - Qf \tag{1}$$

Since Equation 1 for recharge is derived from ET and Qf data, and ET and Qf components are derived from streamflow data, the recharge value estimated does not account for any quantities of recharge transpired by riparian vegetation before reaching the stream. This results in a total recharge that is actually slightly higher than the recharge calculated from the water budget approach. There is no estimation taken into account here of how much the intercepted transpiration value is, which is a limitation to the study. Another limitation is that, like the ET and Qf components of the water budget, the recharge estimate does not account for any interpixel transfers of groundwater. It only accounts for the contribution from precipitation entering each individual cell.

Results and Comparison of results with Reitz et al. (2017)

Based on the procedure above, maps were produced for each water budget component and for the final recharge component. Since a goal of this study was to accurately reproduce recharge rates using the methods presented in Reitz et al. (2017), these maps were visually compared to those of Reitz et al. (2017). General statements are made about any discrepancies between the results of this study and the results of Reitz et al. (2017) and brief explanations are given for those discrepancies. As it is beyond scope of this study to further investigate reasoning for discrepancies, future work will be necessary to resolve them.

RESULTS

Estimating near-present annual groundwater recharge rates

Precipitation

Near-present effective precipitation (precipitation plus groundwater-sourced irrigation) is shown in Figure 9. Regions with the greatest effective precipitation values include the Northwest, Southeast, and Northeast. Regions with the lowest effective precipitation values include the West and Southwest. A divide in precipitation at the 100th meridian is seen at the Great Plains region where lower precipitation values and arid conditions are dominant west of the meridian and higher precipitation values and humid conditions are dominant east of the meridian.

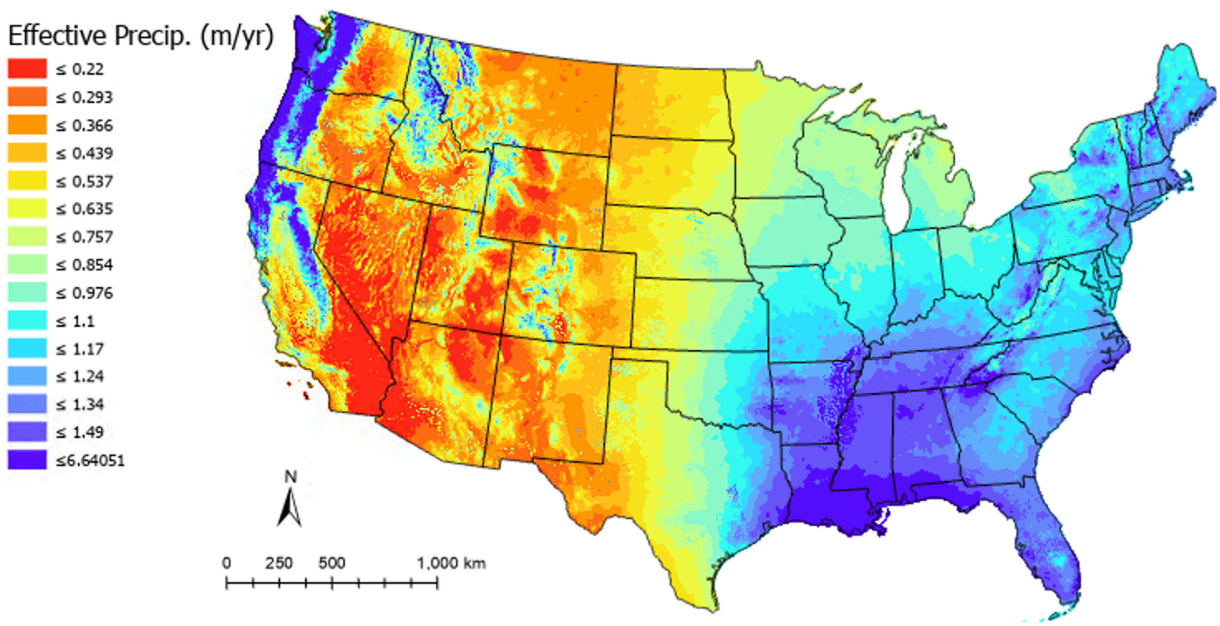

Figure 9. Effective precipitation rates across the CONUS at 800 m resolution. Effective precipitation is equal to precipitation plus groundwater-sourced irrigation.

Evapotranspiration

Near-present evapotranspiration rates, shown in Figure 10, are reflective of an area's temperature, precipitation, and land-cover distribution. Evapotranspiration rates are higher in the eastern half of the CONUS because there is greater precipitation in this area. The western half of the US has overall lower moisture content as a result of the 100th meridian climatic divide, meaning that there is less evapotranspiration occurring overall.

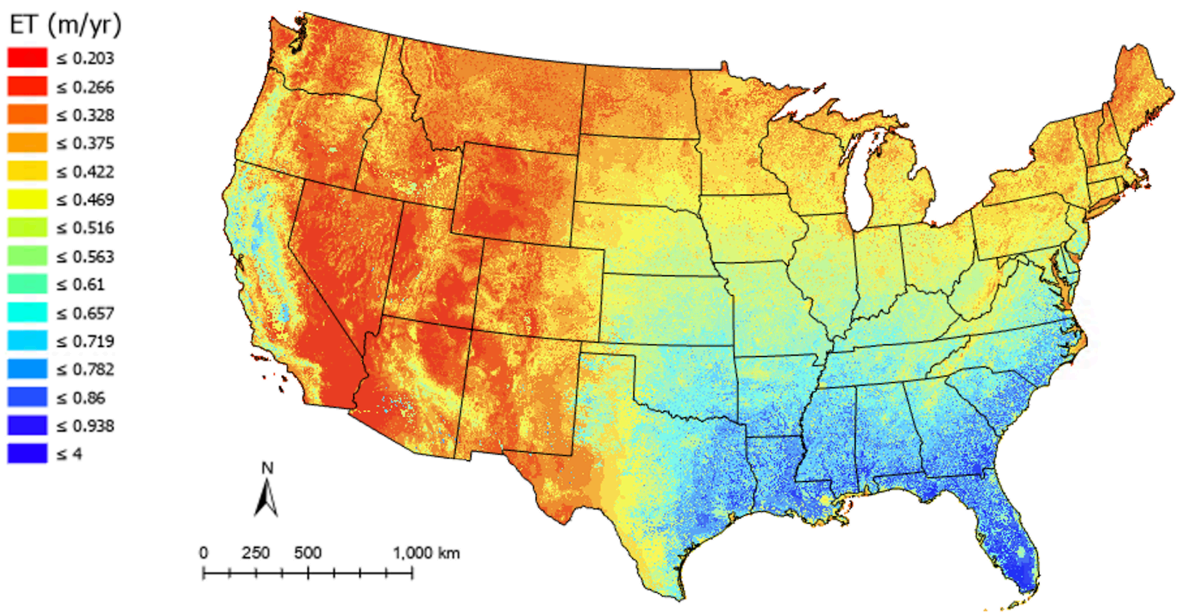

Figure 10. Evapotranspiration rates across the CONUS at 800 m resolution.

Quick flow

Near-present quick flow values, shown in Figure 11, are a reflection of the effective precipitation values and the surficial geology type for any given map area. The patterns seen on the quick flow map are therefore closely related to the patterns seen on the precipitation map (Figure 9). The western half of the US receives less precipitation than the eastern half, so lower quick flow rates over the western US are expected. This pattern again can be attributed to the climatic divide at the 100th meridian.

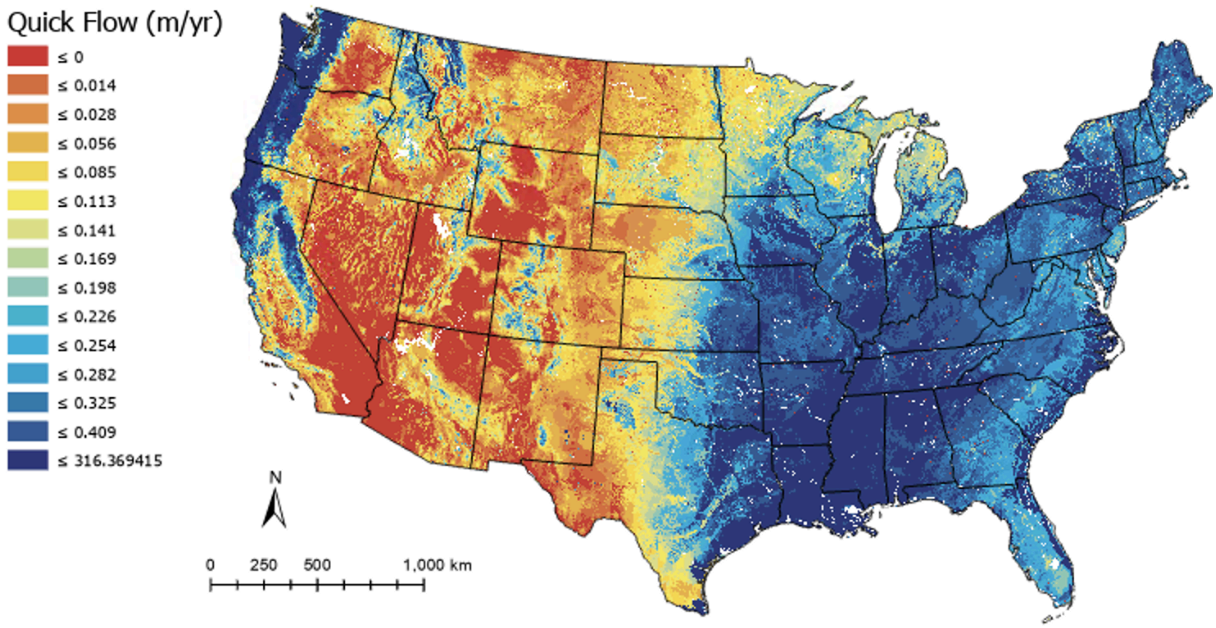

Figure 11. Quick flow runoff across the CONUS at 800 m resolution.

Recharge

Near-present recharge rates, shown in Figure 12, are a result of the water budget equation (Equation 1). Recharge is therefore being influenced by precipitation, evapotranspiration, and quick flow runoff rates. Errors or discrepancies in any of those three water budget components will be carried over as errors in the final recharge values produced. This is important to note because, as presented in the following section, discrepancies between the results produced here and the results produced by Reitz et al. (2017) are present in the evapotranspiration and quick flow runoff water budget components. Errors with the final recharge values produced are therefore also present. Future work involves determining where the discrepancies in the quick flow and evapotranspiration components are coming from and how to resolve them.

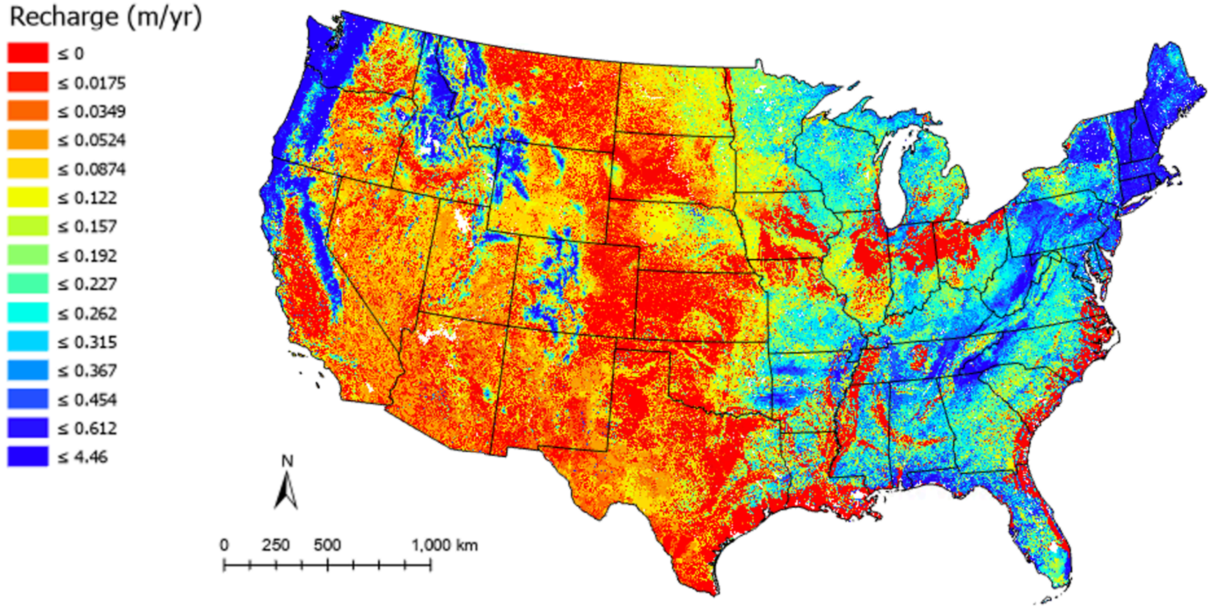

Figure 12. Recharge rates across the CONUS at 800 m resolution.

Comparison of results to Reitz et al. (2017)

Results presented in this study aimed to reproduce those of Reitz et al. (2017). Through visual comparisons of the maps for each water budget component, many similarities are found, along with several discrepancies. Of all water budget components, precipitation is the most similar, likely because it involved using the fewest datasets. In Figure 13, overall visual similarity is high. Differences arise in that values produced by Reitz et al. (2017) are often more towards the extremes than the values produced in this study. For example, minor discrepancies are seen in the southeastern US, where precipitation values produced by Reitz et al. (2017) are higher in some areas than the values produced in this study, and in the southwestern US, where values produced by Reitz et al. (2017) are lower in some areas than the values produced in this study.

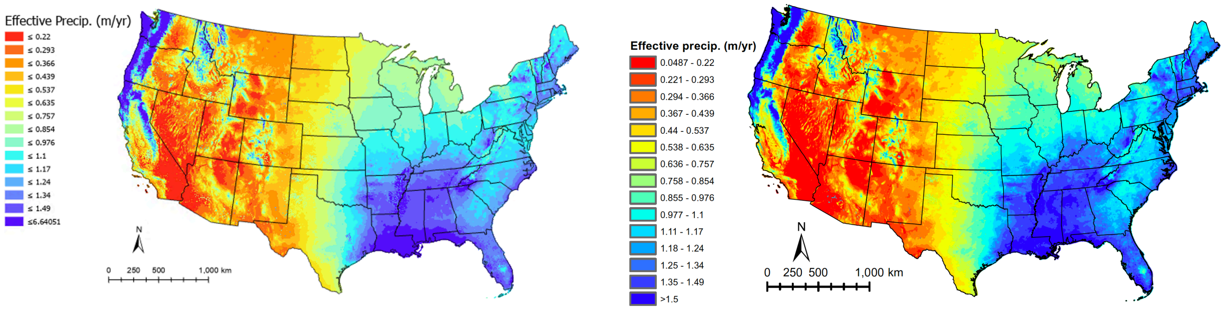

A. B.

Figure 13. Map A is the effective precipitation map produced in this study. Map B is the effective precipitation map produced by Reitz et al. (2017).

The evapotranspiration (ET) water budget component map has some greater differences when compared to the map produced by Reitz et al. (2017; Figure 14). The side-by-side comparison shows that the recharge rates calculated in this study are generally less extreme than those calculated by Reitz et al. (2017). In general, the eastern half has lower evapotranspiration values, and the western half has higher evapotranspiration values than those presented in Reitz et al. (2017). In addition, the map presented in this study appears “grainy”, or as if there are greater differences within regions than there are in reality. For example, looking closely at the southeastern US, it appears blue-green speckled, indicating that there are large shifts in evapotranspiration rates over small areas within this region. In comparison, the southeastern US appears mostly solid blue in the Reitz et al. (2017) version, suggesting little variation in evapotranspiration rates over this region.

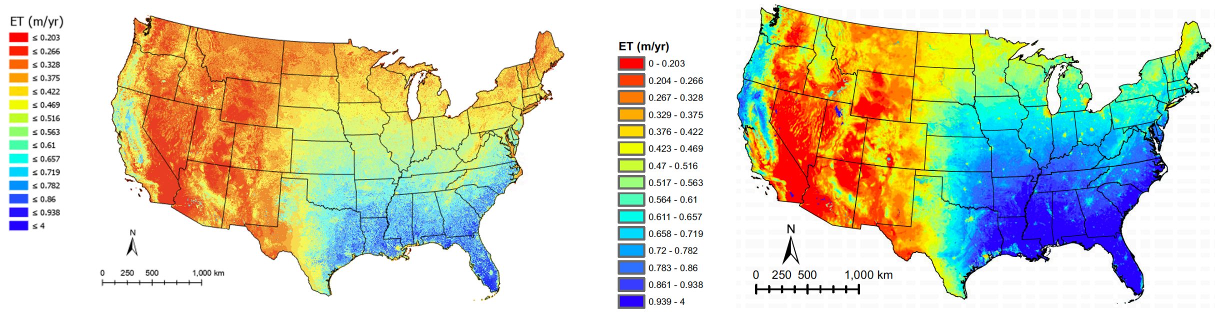

A. B.

Figure 14. Map A is the evapotranspiration map produced in this study. Map B is the evapotranspiration map produced by Reitz et al. (2017).

The quick flow water budget component also has some differences when compared to that of Reitz et al. (2017; Figure 15). The biggest difference is that the values produced in this study are more extreme than the values produced by Reitz et al. (2017). The eastern half of the US has higher values than those in the map from Reitz et al. (2017) and the western half of the US has lower values than those in the map from Reitz et al. (2017). In addition, areas of open water are appearing as having no value (in white) on the map produced in this study, whereas they are appearing as having values in the Reitz et al. (2017) version.

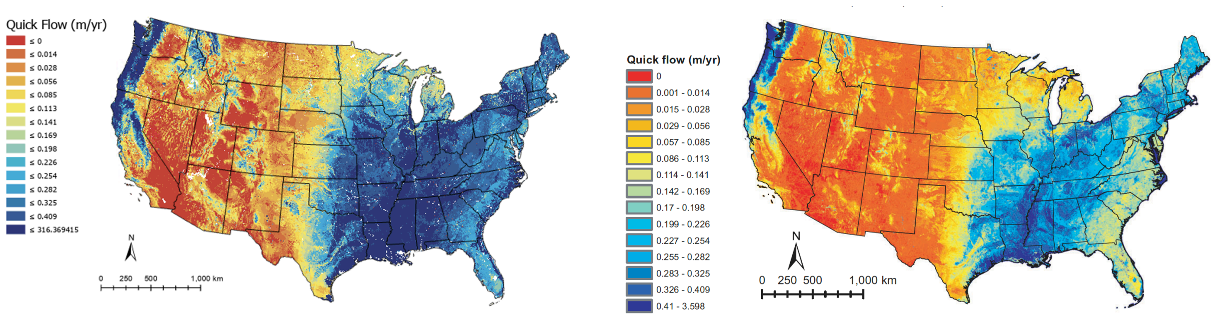

A. B.

Figure 15. Map A is the quick flow map produced in this study. Map B is the quick flow map produced by Reitz et al. (2017).

The final recharge map displays some differences when compared to that of Reitz et al. (2017; Figure 16). This is to be expected because the water budget equation, $R = P - ET - Qf$, indicates that any errors in the P, ET, or Qf components will be carried over as inaccuracies with the final recharge component. Because there were some discrepancies in each of the water budget component maps presented above, discrepancies in the recharge map are expected. As an example, just as in the evapotranspiration map, the recharge map presented in this study appears more "grainy" than the recharge map presented by Reitz et al. (2017), suggesting that this graininess was carried over from the evapotranspiration water budget component. This leads the recharge rates calculated here to appear to vary more drastically within regions than they likely do in reality. In addition, there are several areas across the CONUS that appear to have recharge rates of 0 m/yr, but no regions (except for areas of open water) have 0 m/yr of recharge in the Reitz et al. (2017) version. This discrepancy may be arising in part because of the more extreme values of quick flow calculated in this study than by Reitz et al. (2017; Figure 15). Areas that had very high rates of quick flow are among some of the areas that appear to have very low rates of recharge, such as parts of Ohio, Indiana, and Illinois, as well as much of the Great Plains region.

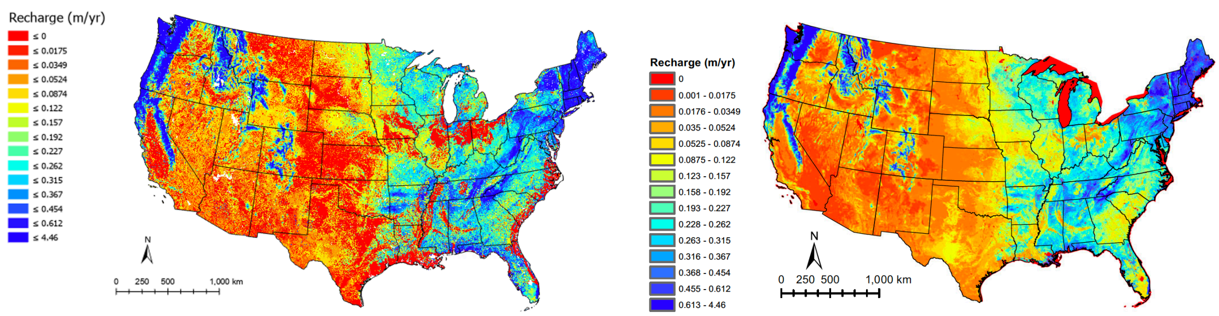

A. B.

Figure 16. Map A is the recharge map produced in this study. Map B is the recharge map produced by Reitz et al. (2017).

DISCUSSION

The future of recharge rates over the Contiguous US

Future groundwater recharge rates across the CONUS can be estimated using the water budget approach presented in this study. Since groundwater recharge rates are dependent on the water budget components of precipitation, quick flow runoff, and evapotranspiration, future patterns of recharge rates can be discussed using predicted trends in these water budget components even without completed calculations of these future water budget components.

Precipitation patterns are closely related to groundwater recharge patterns. It is therefore expected that the changes to precipitation that will occur over the 21st century will impact the availability of water resources. Over the 20th century and through present-day, precipitation over the CONUS has increased by about 4%, although there are some regional and seasonal differences (Easterling et al., 2017). For example, the Midwest has experienced increases in precipitation, but the Southwest has experienced decreases in precipitation. The mechanisms behind changing precipitation patterns are complex, but they can ultimately be tied back to changing large-scale circulation patterns.

Changing precipitation patterns over the Midwest

In the CONUS, several weather types or regimes have been identified as responsible for shaping observed precipitation patterns (Zhang and Villarini, 2019). Weather types are large-scale atmospheric circulation systems that play important roles in shaping weather and climate. Of the several existing weather types that have been identified, the weather type most responsible for providing precipitation to the Midwest includes pressure systems associated with the polar jet stream. The jet stream causes the formation of a high-pressure system over the eastern United States as cold polar air intrudes southward and a low-pressure system over the western United States. The 100th meridian represents the divide between these two systems. The jet stream also separates cold polar air from warm, humid subtropical air. The cold polar air causes the lifting of warm subtropical air, leading to pronounced heavy precipitation over much of the Midwest. This weather type can therefore be summarized as a strong moisture flux transported from the Gulf of Mexico to the Midwest lifted by cold air from the Arctic, leading to heavy frontal precipitation (Zhang and Villarini, 2019).

Over the past several decades, there has been an observed increase in the persistence and frequency of this weather type that influences Midwestern precipitation (Zhang and Villarini, 2019). The threat of heavy and long-lasting precipitation and flooding in the Midwest has therefore gone up in the most recent decades. As precipitation over much of the Midwest is expected to continue to increase into the future, there are some serious implications for the future success of Midwestern farms. Increased precipitation leads to increased soil saturation and degradation. More saturated soils have a lower capacity for groundwater recharge, causing increased runoff rates. Increased runoff then leads to increased land surface erosion and flooding of farmlands. Agricultural production will be negatively affected (Morton et al., 2015).

The United States produces one-third of the world's corn, 70% of which is grown in the Midwest (USDA, 2014). Corn plant development is dependent on the timing and availability of water. Too much rain during the spring may delay planting, impacting the year's productivity, which then impacts the United States' corn output and farmers' profitability. In addition, seeds exposed to too much moisture will germinate and develop too slowly, resulting in unsuccessful plants. In order to ensure the continued productivity of Midwestern farms, farmers will need to make adjustments to farming practices, such as implementing improved drainage systems to ensure that soils stay at an appropriate saturation level. Ecosystem functions association with carbon cycling and water quality will also suffer as a result of increased precipitation frequency and intensity (Morton et al., 2015).

Changing precipitation patterns over the Southwest

Although much of the Midwest will have issues due to receiving too much precipitation, the Southwest will need to deal with the opposite problem of receiving too little precipitation (Easterling et al., 2017). Southwestern agriculture relies heavily on groundwater from the Central Valley aquifer to irrigate crops. Decreases to precipitation due to changing circulation patterns, which leads to decreases to groundwater recharge in the Central Valley aquifer, will limit agricultural production (Elias et al., 2016). In addition to the Central Valley aquifer, snowmelt also provides water for agricultural irrigation especially as snowpack melts gradually during the early half of the growing season. However, diminishing snowpack resources due to warming temperatures is causing an increased reliance on groundwater supplies, placing further stress on the capacity of the Central Valley aquifer (Elias et al., 2016).

Circulation patterns causing increased precipitation to the Midwest are largely controlled by the polar jet stream. In the Southwest, however, the cause of decreased precipitation is more strongly linked to changing tropical circulation patterns of the Hadley Cells. Hadley Cells are circulation cells that have a rising branch of moist air over the equator and a descending branch of dry air at roughly 30° latitude. Descending air suppresses precipitation by drying the lower atmosphere, leading to subtropical dry zones. The effects of the descending branch of the Hadley Cells can be seen in that most of the world's deserts are located around 30° latitude. The southwestern US is located just north of the 30° latitude descending branch of the Hadley Cells, but as the planet warms, Hadley Cells are beginning to expand poleward. For the Southwest, this means that the drying effects of the descending Hadley Cell branch will become increasingly stronger as the subtropical dry zones expand poleward (Seager et al., 2007).

Drying of the Southwest means that agricultural production in the area will suffer. From 1978-2012, a crop yield decline of 11-21% of total irrigated areas was reported (Elias et al., 2016). This crop yield decline was due both to decreasing surface water resources from diminishing snowpack, as well as to decreasing groundwater resources. Drying of the Southwest due to changing circulation patterns affects both snowpack and groundwater resources (Elias et al., 2016).

Future work

The original goals of this project were to (1) accurately reproduce groundwater recharge estimates presented by Reitz et al. (2017) by following their methods and to (2) apply the same methods to estimate future groundwater recharge rates. Given time restraints, only the first goal was addressed in this project. Further work would be necessary to better resolve and assess potential inaccuracies discovered during implementation of the first goal in order to fulfill the second goal.

The next step of this project would be to address the inconsistencies presented in the "Comparing results to Reitz et al. (2017)" section of this project. This involves closely examining how the equations used to calculate evapotranspiration and quick flow rates were entered into the ArcGIS Pro *Model Builder* and the Arcpy Python package. It is likely that small variations in entering these equations could have affected the values produced. It is also possible that the initial input datasets used in this project did not exactly match the datasets used by Reitz et al. (2017), leading to the differences presented above. Because of the limited amount of information presented in the Reitz et al. (2017) methods, the complete evaluation of the results is in question. Future paths to better define the discrepancies would include obtaining the original input datasets of Reitz et al. (2017) and assessing a range of initial inputs to evaluate the sensitivity of this analysis.

Once the near-present water budget components and final recharge rates are more accurately reproduced, the methods may then be applied to estimate groundwater recharge rates for the year 2099 under two RCP scenarios to fulfill the second goal of this project. This step involves downloading NASA Earth Exchange Downscaled Climate Projections (NEX-DCP30) from model runs conducted under the Climate Model Intercomparison Project Phase 5. The RCP scenarios that should be included are the lower emissions scenario RCP4.5 and the higher emissions scenario/business-as-usual scenario RCP8.5. Precipitation and temperature data under these two scenarios will be substituted into the water budget regression equations used in this study.

Under the second goal of the project, a few limitations will present themselves. Certain data needed for the regression equations are not available as future projections, meaning present empirical values for these datasets will be used even when predicting future water budget components. Datasets that do not have future projections available include those describing land-use, land-cover, and irrigation rates. Since land-use, land-cover, and irrigation rates will most definitely change over the 21st century, future recharge estimations will not entirely reflect actual values that will present themselves in the year 2099. In addition, it is always possible that future responses to climate change will not fully align with either of the RCP scenarios that will be used. For this reason, actual future recharge rates may fall outside of or in between the future recharge estimations made using these methods.

Although limitations exist to any results produced using the methods presented here, estimating future groundwater recharge rates will still provide valuable information to water resource planners and the agricultural community. These estimates will allow for preventative measures aimed at avoiding future unsustainable groundwater use to be put in place so that our vital water resources as aquifers can continue to supply water for agriculture and public use.

CONCLUSIONS

This study estimates groundwater recharge rates across the Contiguous US at 800m resolution by reproducing the methods developed by Reitz et al. (2017). This involved using a water budget approach where quick flow runoff and evapotranspiration are subtracted from precipitation. A second goal of this study, although unable to be fulfilled due to time constraints, was to apply these methods to predict groundwater recharge rates at the end of the 21st century by considering CMIP5 precipitation and temperature projections. Since assessing the method's reproducibility was necessary before moving on to project recharge into the future, an assessment of the model's reproducibility is presented here. In addition, since likely changes to future groundwater recharge rates will correspond with future changes to precipitation patterns, the precipitation patterns that govern different parts of the CONUS are examined.

Some aspects of the model were found to be more reproducible than others. The precipitation component of the water budget was the most similar to the corresponding precipitation component presented by Reitz et al. (2017). The quick flow component and the evapotranspiration component, on the other hand, were found to have some greater differences between their corresponding versions in Reitz et al. (2017). For example, the results of this study show more extreme values of quick flow over all parts of the US, with the western half of the country displaying lower values and the eastern half of the country displaying higher values than the Reitz et al. (2017) version. For the evapotranspiration component, values appear overall less extreme and the whole map has a "grainy" appearance, suggesting greater variation within regions than there is according to the Reitz et al. (2017) version. Since recharge is calculated with a water budget approach, any inaccuracies developed in any of the three water budget components – precipitation, quick flow runoff, and evapotranspiration – would be carried over as inaccuracies in the final recharge map. The final recharge map does indeed have drastic differences compared to that of Reitz et al. (2017) due to inaccuracies being carried over from the first three water budget components.

As a way of estimating changes to future groundwater recharge rates, precipitation patterns and the atmospheric circulation systems that govern them are presented for the Midwest and for the Southwest. Overall, the Midwest is becoming wetter, while the Southwest is becoming drier. Changes to recharge in these regions due to changing precipitation patterns have large implications for future agricultural production. The most obvious worry for negative impacts to agricultural production comes from the observed drying of the Southwest, where 40% of the country's fruit is produced using groundwater irrigation from the Central Valley aquifer (USGS, 2020). Unsustainable depletion of the Central Valley aquifer and the resulting water shortages threatens fruit production capacity. However, an increasingly wetter Midwest has the capabilities to cause just as much damage to agricultural systems for a region that produces 70% of the country's corn (USDA, 2014). Corn production relies on the timing and availability of water, where too much rain in the spring leads to late planting, and too-saturated soils prevent the healthy germination and development of corn plants.

Projecting future recharge rates, which is a future goal of this study, is important for providing water resource managers with reliable and region-specific information on the future availability of water. Future climate change scenarios can be used to explore the range of possible changes to groundwater resources, which have immense importance in the country's food production. The current threats to our agricultural system indicate that regions that produce significant amounts of our country's foods are going to suffer as changes to precipitation patterns intensify into the future. Providing high-resolution maps of the range of possible future recharge rates has the capacity to demonstrate to water resource managers the importance of making changes to current water-use practices now in order to protect agricultural production in the future.

APPENDICES

Appendix A

Python script used to calculate evapotranspiration rates over the CONUS with ArcGIS Pro's Arcpy Python package is presented here alongside a description of each step.

The ET equation (Equation 3) is:

$$\frac{ET}{P} = \frac{\Lambda(\frac{\Delta T}{\Delta \overline{T}})(\frac{T+C_1}{\overline{T}+C_1})^2}{\left(\frac{\Delta T}{\Delta \overline{T}}\right)\left(\frac{T+C_1}{\overline{T}+C_1}\right)^2 + (\frac{P}{\overline{P}})^{\frac{3}{2}}}$$

Where $\Lambda = 1 + aL_u + bL_f + cL_s + dL_g + fL_a + gL_m$ (Equation 4) describes land-cover distribution.

Python Script	Description
from arcpy import env from arcpy.sa import * envWrkSpc=env.workspace print(envWrkSpc) arcpy.CheckOutExtension("Spatial")	Importing necessary libraries, setting up environment, and checking out the Spatial extension
urban10_in=Raster("urban10") marsh10_in=Raster("marsh10") forest10_in=Raster("forest10") grassland10_in=Raster("grassland10") shrubs10_in=Raster("shrubs10") agriculture10_in=Raster("agriculture10")	Bringing in Boolean rasters for the Λ land-cover distribution component
prism_tmean_in=Raster("prism_tmean_2000_2013") prism_deltat_in=Raster("prism_deltat") eff_precip2_in=Raster("eff_precip2")	Bringing in rasters for mean temperature, change in temperature, and effective precipitation
val1=13.1366303	Value of $\Delta\overline{T}$
val2=11.410199	Value of $\overline{T}$
val3=0.808699	Value of $\overline{P}$
valC1=15.9	Value of C_1 fitting coefficient

vala=0.0526	Value of the fitting coefficient for the urban land-cover type
valb=0.242	Value of the fitting coefficient for the forest land-cover type
valc=-0.0106	Value of the fitting coefficient for the shrub land-cover type
vald=0.236	Value of the fitting coefficient for the grassland land-cover type
valf=0.352	Value of the fitting coefficient for the agriculture land-cover type
valg=0.520	Value of the fitting coefficient for the marsh land-cover type
term1=1+(vala*urban10_in)+(valb*forest10_in)+(valc*shrubs10_in)+(vald*grassland10_in)+(valf*agriculture10_in)+(valg*marsh10_in) term2=prism_deltat_in/val1 term3=((prism_tmean_in+valC1)/(val2+valC1))**2 term4=prism_deltat_in/val1 term5=((prism_tmean_in+valC1)/(val2+valC1))**2 term6=(eff_precip2_in/val3)**(3/2)	Calculating each term of Equation 4
outValue=((term1*term2*term3)/((term4*term5)+term6))*eff_precip2_in	Calculating the final ET value

Appendix B

The *Model Builder* feature in ArcGIS Pro was used to execute Equation 5 for calculating quick flow runoff rates: $R_g = C_1 g \left(\frac{P}{\bar{P}}\right)^{a_g} (\frac{K}{\bar{K}})^{b_g} + C_2 g$

A screen capture of the model is presented here. Each of the 16 different surficial geology types considered in the quick flow component have unique values for each fitting parameter in Equation 5 ($C_1 g$, a_g, b_g, and $C_2 g$), which are presented in Table 1. Therefore, using the *Model Builder* made it possible to store the 16 versions of the equation to allow the entire quick flow component to be run with one command (Appendix B-1).

The output of running the model was 16 new layers for quick flow rates for each surficial geology type, each displaying quick flow for across the entire CONUS. Since each quick flow rate output should only be applied to the areas of the CONUS with the corresponding surficial geology type, each output layer was multiplied by a Boolean raster that had “1” for areas with a given surficial geology type and “0” for areas that did not have that given surficial geology type. The resulting layers were then added together using the *Raster Calculator* tool to produce a final quick flow map that displayed the appropriate quick flow values for each area of the CONUS based on an area’s given surficial geology type.


```
0.2021 * (( "%eff_precip2%" /0.80228) ** 1.452)
* (( "%STATSGO_PolygonToRaster%" /19.012265) **
(-0.2629)) - 0.05542
```

Appendix B-1.

REFERENCES CITED

California Department of Water Resources, 2020, California Marks Key Step Toward Achieving Sustainable Groundwater Management: https://water.ca.gov/News/News-Releases/2020/CA-Marks-Key-Step-Toward-Achieving-Sustainable-Groundwater-Management (accessed February 2021).

Easterling, D.R., Kunkel, K.E., Arnold, J.R., Knutson, T., LeGrande, A.N., Leung, L.R., Vose, R.S., Waliser, D.E., and Wehner, M.F., 2017, Precipitation change in the United States In: Climate Science Special Report: Fourth National Climate Assessment, Volume I [Wuebbles, D.J., Fahey, D.W., Hibbard, K.A., Dokken, D.J., Stewart, B.C., and Maycock, T.K. (eds.)]. U.S. Global Change Research Program, Washington, DC, USA, p. 207-230, doi: 10.7930/J0H993CC.

Elias, E., Rango, A., Smith, R., Maxwell, C., Steele, C., Havstad, K., 2016, Climate change, agriculture and water resources in the Southwestern United States: Journal of Contemporary Water Research and Education, v. 158, p. 46-61, doi:10.1111/j.1936-704X.2016.03218.x.

IPCC, 2013: Climate Change 2013: The Physical Science Basis. Contribution of Working Group I to the Fifth Assessment Report of the Intergovernmental Panel on Climate Change [Stocker, T.F., D. Qin, G.-K. Plattner, M. Tignor, S.K. Allen, J. Boschung, A. Nauels, Y. Xia, V. Bex and P.M. Midgley (eds.)]. Cambridge University Press, Cambridge, United Kingdom and New York, NY, USA, 1535 pp.

Lamont-Doherty Earth Observatory, 2018, The 100th meridian, where the Great Plains begin, may be shifting: https://www.ldeo.columbia.edu/news-events/100th-meridian-where-great-plains-begin-may-be-shifting (accessed January 2021).

Morton, L. W, Hobbs, J., Arbuckle, J. G., Loy, A., 2015, Upper Midwest climate variations: Farmer responses to excess water risks: Journal of Environmental Quality, v. 44, p. 810-822, doi: 10.2134/jeq2014.08.0352.

Mrad, A., Katul, G. G., Levia, D. F., Guswa, A. J., Boyer, E. W., Bruen, M., Carlyle-Moses, D. E., Coyte, R., Creed, I. F., van de Giesen, N., Grasso, D., Hannah, D. M., Hudson, J. E., Humphrey, V., Iida, S., Jackson, R. B., Kumagai, T., Llorens, P., Michalzik, B., Nanki, K., Peters, C. A., Selker, J. S., Tetzlaff, D., Zalewski, M., Scanlon, B. R., 2020, Peak grain forecasts for the US High Plains amid withering waters: Proceedings of the National Academy of Sciences of the United States of America, v. 117, p. 26145-26150, doi: 10.1073/pnas.2008383117.

NASA, 2021, 2020 Tied for Warmest Year on Record, NASA Analysis Shows: https://www.nasa.gov/press-release/2020-tied-for-warmest-year-on-record-nasa-analysis-shows (accessed February 2021).

NLCD, 2020, Multi-resolution Land Characteristics Consortium: https://www.mrlc.gov/data (accessed October 2020).

Pielke, R. A. Sr., Pitman, A., Niyogi, D., Mahmood, R., McAlpine, C., Hossain, P., Goldewijk, K. K., Nair, U., Betts, R., Fall, S., Reichsten, M., Kabat, P., and de Noblet, N., 2011, Land use/land cover changes and climate: modeling analysis and observational evidence: WIREs Climate Change, v. 2, p. 828-850, doi: 10.1002/wcc.144.

Purdue Policy Research Institute, 2018, Global Drivers of Land and Water Sustainability Stresses at Mid-century: https://docs.lib.purdue.edu/cgi/viewcontent.cgi?article=1017&context=gpripb (accessed September 2020).

Reitz, M., Sanford, W. E., Senay, G. B., Cazenas, J., 2017, Annual estimates of recharge, quick-flow runoff, and evapotranspiration for the Contiguous U.S. using empirical regression equations: Journal of the American Water Resources Association, v. 54, p. 961-983, doi:10.1111/1752-1688.12546.

Scanlon, B. R., Faunt, C. C., Longuevergne, L., Reedy, R. C., Alley, W. M., McGuire, V. L., McMahon, P. B., 2012, Groundwater depletion and sustainability of irrigation in the US High Plains and Central Valley: Proceedings of the National Academy of Sciences of the United States of America, v. 109, p. 9320-9325, doi:10.1073/pnas.1200311109.

Seager, R., Feldman, J., Lis, N., Ting, M., Williams, A. P., Nakamura, J., Liu, H., Henderson, N., 2018, Whither the 100th Meridian? The once and future physical and human geography of Amercia's arid-humid divide: Part II: The meridian moves east: Earth Interactions, v. 22, p. 1-24, doi:10.1175/EI-D-17-0012.1.

Seager, R., Ting, M., Held, I., Kushnir, Y., Lu, J., Vecchi, G., Huang, H., Harnik, N., Leetmaa, A., Lau, N., Li, C., Velez, J., Naik, N., 2007, Model projections of an imminent transition to a more arid climate in Southwestern North America: Science, v., 316, 1181-1184, doi:10.1126/science.1139601.

United States Geological Survey (USGS), 2015, The quality of the Nation's groundwater: https://www.usgs.gov/news/quality-nation's-groundwater (accessed October 2020).

United States Geological Survey (USGS), 2020, California's Central Valley regional characteristics: https://ca.water.usgs.gov/projects/central-valley/about-central-valley.html (accessed October 2020).

USDA, 2014, Crop production: http://www.usda.gov/wps/portal/usda/usdahome?parentnav=AGRICULTURE&navid=CROP_PRODUCTION&navtype=RT (accessed February 2021).

USDA, 2019, Web Soil Survey: http://websoilsurvey.nrcs.usda.gov (accessed October 2020).

U. S. Global Change Research Program, 2018, Fourth National Climate Assessment Volume II: https://nca2018.globalchange.gov/downloads/NCA4_2018_FullReport.pdf (accessed October 2020).

Vose, R.S., Easterling, D.R., Kunkel, K.E., LeGrande, A.N., and Wehner, M.F., 2017, Temperature changes in the United States In: Climate Science Special Report: Fourth National Climate Assessment, Volume I [Wuebbles, D.J., Fahey, D.W., Hibbard, K.A., Dokken, D.J., Stewart, B.C., and Maycock, T.K. (eds.)]. U.S. Global Change Research Program, Washington, DC, USA, pp. 185-206, doi:10.7930/J0N29V45.

Zhang, W., and Villarini, G., 2019, On the weather types that shape the precipitation patterns across the U.S. Midwest: Climate Dynamics, v. 53, p. 4217-4232, doi:10.1007/s0038 2-019-04783 -4.